International Journal of Nanomedicine

Dovepress
open access to scientific and medical research

Open Access Full Text Article

ORIGINAL RESEARCH

Co-delivery of everolimus and vinorelbine via a tumor-targeted liposomal formulation inhibits tumor growth and metastasis in RCC

This article was published in the following Dove Press journal:
International Journal of Nanomedicine

Krishnendu Pal*
Vijay Sagar Madamsetty*
Shamit Kumar Dutta
Debabrata Mukhopadhyay

Department of Biochemistry and Molecular Biology, Mayo Clinic Florida, Jacksonville, FL 32224, USA

*These authors contributed equally to this work

Background: Renal cell carcinoma (RCC) is notorious for its resistance towards chemotherapy and radiation therapy in general. Combination therapy is often helpful in alleviating the resistance mechanisms by targeting multiple signaling pathways but is usually more toxic than monotherapy. Co-encapsulation of multiple therapeutic agents in a tumor-targeted drug delivery platform is a promising strategy to mitigate these limitations.

Methods: A tumor-targeted liposomal formulation was prepared using phospholipids, cholesterol, DSPE-$(PEG)_{2000}$-OMe and a proprietary tumor-targeting-peptide (TTP)-conjugated lipopeptide. An efficient method was optimized to encapsulate everolimus and vinorelbine in this liposomal formulation. Single drug-loaded liposomes were also prepared for comparison. Finally, the drug-loaded liposomes were tested in vitro and in vivo in two different RCC cell lines.

Results: The tumor-targeted liposomal formulation demonstrated excellent tumor-specific uptake. The dual drug-loaded liposomes exhibited significantly higher growth inhibition in vitro compared to the single drug-loaded liposomes in two different RCC cell lines. Similarly, the dual drug-loaded liposomes demonstrated significantly higher suppression of tumor growth compared to the single drug-loaded liposomes in two different subcutaneous RCC xenografts. In addition, the dual drug-loaded liposomes instigated significant reduction in lung metastasis in those experiments.

Conclusion: Taken together, this study demonstrates that co-delivery of everolimus and vinorelbine with a tumor-targeted liposomal formulation is an effective approach to achieve improved therapeutic outcome in RCC.

Keywords: liposomes, combination therapy, everolimus, vinorelbine, renal cancer, metastasis

Introduction

The prevalence of kidney cancer is continuing to rise steadily over the past few decades. About 65,340 new diagnoses and 14,970 deaths due to kidney cancer are projected in the United States in 2018.[1] Renal cell carcinoma (RCC) accounts for approximately 90% of all kidney cancers.[2] Among them, clear cell renal cell carcinoma (ccRCC) is the most prevalent (75–80%) subtype of RCC.[3] Papillary RCC (10–16%) and chromophobe RCC (5%) represent the most common remaining histologic subtypes.[3] Traditional chemotherapy and radiation therapy are largely ineffective in the treatment of all RCC subtypes.[4,5] The bleak situation could not be improved significantly even after the advent of immunotherapy since it was effective only in

Correspondence: Debabrata Mukhopadhyay
Department of Biochemistry and Molecular Biology, Griffin 411, Mayo Clinic Florida, 4500 San Pablo Road S, Jacksonville, FL 32224, USA
Tel +1 904 953 6177
Email mukhopadhyay.debabrata@mayo.edu

http://doi.org/10.2147/IJN.S204221

a minority of patients.[6,7] Although, tyrosine kinase inhibitors (TKI) such as sunitinib, pazopanib and sorafenib; mTOR inhibitors such as everolimus, temsirolimus; and anti-VEGF–humanized antibody bevacizumab are now used as standard first- and second-line therapy for RCC, enduring treatment response is still without reach.[8–10]

Combination therapy is the most actively pursued approach of present day antitumor therapy. Combinatorial drug treatments typically exert their effect through the inhibition of several signaling pathways or multiple nodes in a single signaling cascade.[11] The benefits of combination therapy are well documented by a plethora of clinical studies demonstrating synergistic effects greater than the sum of the therapeutic outcomes of each drug.[12–15] Unfortunately, not many combination therapies are successful in RCC especially advanced metastatic RCC. The combination of VEGF-targeted therapy and mTOR inhibitors, while effective in animal models,[16,17] produced unsatisfactory results in randomized trials.[18–20] In fact, the combination of sunitinib and mTOR inhibitors (everolimus or temsirolimus) demonstrated significant toxicity in separate Phase I trials.[21,22] However, significant improvement in progression-free survival and overall survival was observed in a recent Phase II trial in second-line combination treatment with everolimus plus lenvatinib (a novel TKI) compared to the everolimus monotherapy.[23] Bevacizumab plus interferon-alfa in first-line setting[24] and lenvatinib plus everolimus as second-line treatment[23] are among the first approved combination therapies for RCC. Recently, Food and Drug Administration and the European Medicines Agency approved the combination of two immune checkpoint inhibitors, nivolumab and ipilimumab, as the new standard of care treatment for intermediate- and poor-risk patients, as the combination demonstrated better efficacy than sunitinib.[25] In addition, two separate large Phase III trials demonstrated the superiority of avelumab (a programmed death ligand 1 inhibitor) plus axitinib and pembrolizumab (a programmed death 1 inhibitor) plus axitinib over sunitinib with respect to progression-free survival and the objective response rate.[26,27] Pembrolizumab plus axitinib showed an improved overall survival as well. Both these combinations are anticipated to become new standards of care treatments for RCC. Nonetheless, the dosage of each individual drug is often needed to be reduced in the combination regimen due to increased toxicity, which severely limits the benefits otherwise achievable from this approach.[28] Undoubtedly, there is an unmet need for an ideal drug delivery platform capable of delivering multiple drugs in a tumor-specific manner and reducing their systemic toxicity.

Among the numerous platforms available for drug delivery, liposomes offer great promise since they possess quite a few unique characteristics. First, liposomes can entrap both lipophilic and hydrophilic compounds which allow the encapsulation of an assortment of drugs having different solubility.[29] The liposomes also help to protect the encapsulated drugs from chemical inactivation, enzymatic degradation or immunological neutralization, and thereby preserve the potency of drugs until they are delivered to the target tissues.[30] The surface of the liposomes can be grafted with polyethylene glycols in order to prolong the circulating half-lives of drugs, which, in turn, results in significantly higher accumulation of liposomal drugs in tumors compared to normal tissues via enhanced permeability and retention (EPR) effect.[31] Decorating the liposome surface with a tumor-targeting ligand also improves the tumor-specific accumulation, albeit in a more active manner.[32] Consequently, liposomal drug formulations elicit considerably less drug-induced toxicity.[33] In addition, liposomes demonstrate excellent biocompatibility and minimal immune reactivity.[34] All these aspects contribute towards an improved therapeutic index of a drug in the liposomal formulation. Quite a few liposomal drug formulations including Doxil®, DaunoXome®, Depocyt®, Myocet®, Mepact®, Marqibo® and Onivyde® are currently being used in the clinics.[35] However, to the best of our knowledge, no FDA-approved liposomal formulation utilizes active targeting by means of a targeting ligand.

Here we report the development of a liposomal formulation decorated with a novel tumor-targeted peptide (TTP) and its utilization for targeted delivery of everolimus and vinorelbine in RCC xenografts. We have selected this particular combination based on our previous study where we had shown that the therapeutic efficacy of vinorelbine in RCC was enhanced in combination with antiangiogenic therapy with a VEGF-neutralizing antibody.[36] Interestingly, in addition to its role in metabolism, everolimus demonstrates antiangiogenic properties as well.[37,38] Consequently, we hypothesized that the combination of everolimus and vinorelbine would work in a similar way to enhance the efficacy of vinorelbine, and the metabolism-regulatory activity of everolimus would be an added advantage compared to the previous study. In addition, the lipophilicity of everolimus and hydrophilicity of vinorelbine would ensure their separate

spatial distribution inside the liposomes resulting in increased drug loading efficiency. Nonetheless, our results demonstrate that the TTP-liposomes have excellent tumor-targeting efficacy and are capable of encapsulating multiple drugs. We further analyzed the efficacy of TTP-liposomes loaded with everolimus and vinorelbine in inhibiting proliferation in vitro and tumor growth and lung metastasis in vivo in two different RCC cell lines. Taken together, this study presents the synthesis, characterization and evaluation of a dual drug-loaded tumor-targeted liposomal formulation in RCC xenografts with the long-term goal of translating the findings for the betterment of RCC patients.

Materials and methods

Reagents

DOPC was purchased from Avanti Polar Lipids. DSPE-$(PEG)_{2000}$-OMe was purchased from Nanosoft Polymers. Cholesterol was purchased from Sigma. Everolimus was purchased from LC laboratories. Vinorelbine was purchased from Fisher Scientific. Ki67 antibody was purchased from Abcam.

Cell culture

786-O and A498 cells were purchased from American Type Culture Collection. No authentication of the cell lines was done by the authors. Cells were maintained in Dulbecco's modified Eagle medium (DMEM; Life Technologies) supplemented with 10% fetal bovine serum (FBS; Fisher Scientific) and 1% penicillin–streptomycin (Invitrogen) at 37°C in a humidified atmosphere with 5% CO_2. Cultures of 85–90% confluency were used for all of the experiments.

Synthesis of TTP-conjugated lipopeptide

TTP (a tumor-targeting-peptide with a proprietary sequence)-conjugated lipopeptide was synthesized using Fmoc-strategy-based solid phase peptide synthesis method. Briefly, Wang resin preloaded with Fmoc-protected C-terminal amino acid (in the proprietary sequence of TTP) was swollen in DMF for 30 mins. Then, excess DMF was drained and Fmoc deprotection was carried out by suspending the resin particles in 20% piperidine in DMF and agitating them for 15 mins by bubbling nitrogen gas through the suspension. The resin was then sequentially washed with 3 changes of DMF, 2 changes of methanol and again 2 changes of DMF. After final DMF wash, sequential coupling of the amino acid residues (from C-terminal to N-terminal) was performed using standard solid phase synthesis procedure. Each coupling of an amino acid residue involved addition of the appropriate Fmoc-amino acid (two equivalents) pre-activated with HBTU (two equivalents); HOBT (two equivalents) and DIPEA (four equivalents) in DMF to the resin (one equivalent) and agitation of resin particles by nitrogen bubbling for 3 hrs. Then, the resin was washed with two changes of DMF and Fmoc deprotection was carried out as described earlier. These steps were repeated until the TTP amino acid sequence was completed. Then, the peptide was PEGylated by conjugating Fmoc-$(PEG)_n$-CO_2H in similar fashion. Following Fmoc deprotection, the resin containing PEGylated peptide was reacted with succinic anhydride (4 equivalents) and DMAP (4 equivalents) overnight. Excess reagents were washed off with 2 changes of DMF and the resin containing terminal succinic acid group was activated with HBTU (2 equivalents), HOBT (2 equivalents) and DIPEA (4 equivalents) in DMF for 30 min followed by DMF washes and addition of the lipid moiety (N,N-di-n-octadecyl-N-2-aminoethylamine) (2 equivalents). The resin was allowed to agitate overnight. Finally, the resin was sequentially washed with DMF, methanol and DCM (3 changes each). Peptide cleavage from the resin as well as global deprotection was carried out by treating the resin on ice with a solution consisting of TFA, water, thioanisole and triisopropylsilane, in a volume ratio of 85:5:5:5 for 4 hrs. The volatile components were removed with nitrogen flush and under reduced pressure to obtain the crude solid lipopeptide which was further purified by ether precipitation to remove soluble impurities. The precipitated lipopeptide was collected by centrifugation, dried and kept at −20°C until further use.

Preparation of empty liposomes

Liposomes were prepared by a modified ethanol injection method.[39] An ethanolic solution of required amounts of TTP-conjugated lipopeptide, phospholipids and cholesterol was warmed in a 65°C water bath for 5 mins and injected slowly into milli-Q water pre-heated to 65°C under magnetic stirring. Spontaneous liposome formation occurred as soon as ethanolic lipid solution was in contact with the aqueous phase. Stirring was continued for 15 mins at room temperature. Then, ethanol and a part of water were removed by rotary evaporation under reduced pressure and volume was made up with milli-Q water.

Preparation of drug-loaded liposomes

Drug-loaded liposomes were prepared as described earlier. A schematic representation has been displayed in Figure 1A.

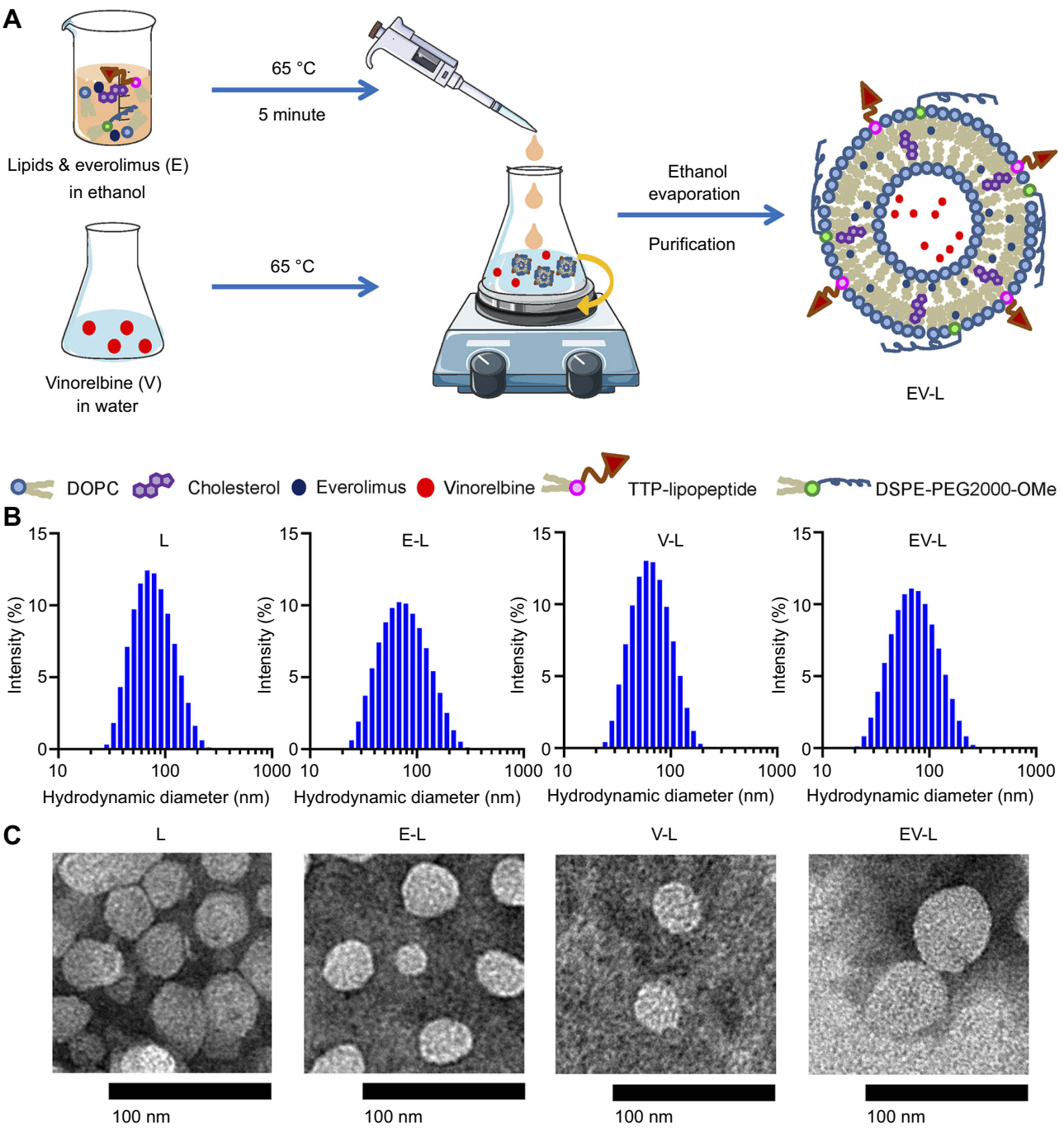

Figure 1 Synthesis and characterization of drug-loaded liposomes. (**A**) Schematic representation of the synthesis of drug-loaded liposomes. (**B**) Hydrodynamic diameter histograms of respective liposomes obtained from DLS intensity measurements. (**C**) Representative TEM images of respective liposomes. Bar Length =100 nm.
Abbreviations: DOPC, 1,2-dioleoyl-sn-glycero-3-phosphocholine; TTP, tumor targeting peptide; DSPE-PEG2000-OMe, 1,2-distearoyl-sn-glycero-3-phosphoethanolamine-N-[methoxy(polyethylene glycol)-2000] (ammonium salt).

The hydrophilic drug vinorelbine was added to the aqueous phase, while the lipophilic drug everolimus was added to the ethanolic solution of lipids. Both single drug and combined drug-loaded liposomes were prepared. Unentrapped drugs were removed by amicon ultra centrifugal filters with a cut off size of 3 kD. The obtained liposome concentrates were collected; volume was made up with milli-Q water and the liposomes were stored at 4°C.

Liposome size and zeta potential analysis

Mean hydrodynamic diameter and zeta potential of empty and drug-loaded liposomes were determined by dynamic

light scattering (DLS) measurements using a Malvern Zetasizer (Malvern, UK), after sample dilution in deionized water. All measures were performed in triplicate at 25°C.

Analysis of drug loading and encapsulation efficiency

Liposome-encapsulation efficiency was measured by determining the amount of entrapped drugs. Briefly, the drug-loaded liposome sample was centrifuged in an amicon ultra centrifugal filter with a cut off size of 3 kD in order to separate the unentrapped drug. Total (T_{drug}) and unentrapped drug (UE_{drug}) amounts were determined by high-performance liquid chromatography (HPLC) measurements and comparing with corresponding standard curves. The encapsulated drug (E_{drug}) amount was calculated by subtracting the amount of unentrapped drugs (UE_{drug}) from total drug (T_{drug}) amount. The drug encapsulation efficiency (EE) was expressed as the percentage of the encapsulated amount (E_{drug}) to the total amount (T_{drug}). The drug loading efficiency (DLE) was calculated as the percentage of the encapsulated amount (E_{drug}) to the total lipid amount (T_{lipid}).

In vitro cellular uptake of liposomes

Cellular uptake was investigated by using Rhodamine-PE-labeled fluorescent liposomes by means of EVOS FL Auto fluorescence microscope. Toward this aim, some liposome suspensions were prepared by adding Rhodamine-PE (Avani Polar Lipids) to the organic phase. 786-O and A498 human clear cell renal cell carcinoma (ccRCC) cells were grown on 96 well plates at a density of 1×10^4 cells/well for 24 hrs at 37°C. Then, the cells were incubated in the presence of fluorescent liposomes for 4 hrs. A control liposome (CL) without any targeting peptide was used to discern the targeting efficiency. Nuclei of the cells were counterstained with Hoechst for the last 30 mins. After 4 hrs of incubation in the presence of the fluorescent liposomes, the cells were rinsed with PBS (pH 7.4) three times and then overlaid with 100 µL PBS. The cells were immediately imaged with EVOS FL Auto fluorescent microscope under bright field, blue, and red channel.

In vivo biodistribution of liposomes

Six- to eight-week-old male SCID mice were obtained from in house breeding and housed in the institutional animal facilities. All animal work was performed following Association for Assessment and Accreditation of Laboratory Animal Care (AAALAC) guidelines under protocols approved by the Mayo Clinic Institutional Animal Care and Use Committee. To establish tumor growth in mice, 5×10^6 786-O or A498 cells, resuspended in 100 µL of 50% matrigel in PBS, were injected subcutaneously into the right flank. Tumors were allowed to grow for 6–7 weeks without treatment until the average size of tumors reached 300–500 mm^3. Then, either control (CL) or targeted (TL) liposomes containing IR-780-Dye were administered via intravenous route. Mice were imaged using IVIS imager 24 and 48 hrs after administration. Finally, mice were sacrificed; tumors and major organs were collected and imaged.

In vitro cytotoxicity assay

Approximately, 5×10^3 cells were seeded in 96-well plates. After 24 hrs, cells were treated with increasing doses of empty liposome or liposomes containing everolimus, vinorelbine and a combination thereof diluted in respective media and incubated for further 72 hrs. At the end of the incubation, cell viability was measured using Celltiter 96 Aqueous One Solution Cell Proliferation Assay (Promega) as per the manufacturer's protocol. Briefly, the media containing the treatments were aspirated from the plate and washed with PBS. Then, 100 µL media containing 20 µL One Solution reagent was added to each well. The plate was incubated at 37°C for 30 mins and absorbance at 492 nm was measured using Spectramax i3x. Percentage viability is calculated as follows:

$$\text{Viability}\,(\%) = 100 \times (A_{\text{Treated}} - A_{\text{Blank}})/(A_{\text{Untreated}} - A_{\text{Blank}}).$$

In vivo tumor regression experiment

A single mouse trial (SMT) was used to assess the in vivo tumor regression efficacy of the drug-loaded liposomes in 786-O xenografts as described previously.[40–46] Mice with ~300–500 mm^3 tumors were treated with empty liposome, liposome containing everolimus, vinorelbine and a combination of both three times a week via intravenous route. The liposome amount among treatments was kept constant in such a way that the E-Liposome and EV-Liposome treated mouse gets 20 µg of Everolimus each. Tumors were measured weekly and plotted to obtain a tumor growth curve. After completion of experiment, all tumor-bearing mice were euthanized with CO_2; tumors were removed, weighed and prepared for immunochemistry. The single mouse trial with key treatment groups was repeated in A498 xenografts. To validate the results obtained from the

SMT, we repeated the experiment in cohorts of 5 mice per group with the most effective treatment group and vehicle control in 786-O tumor-bearing mice.

Immunohistochemistry

Tumors and organs were removed and fixed in neutral buffered 10% formalin at room temperature for 24 hrs before embedding in paraffin and sectioning. Sections were deparaffinized and then subjected to hematoxylin and eosin (H&E), and Ki67 immunochemistry according to the manufacturer's instructions (DAB 150; Millipore). Stable diaminobenzidine was used as a chromogen substrate, and the sections were counterstained with a hematoxylin solution. Photographs of the entire cross-section were digitized using Aperio AT2 slide scanner (Leica). Images were analyzed using Imagescope software (Leica).

Statistical methods

The independent-samples *t*-test was used to test the probability of significant differences between groups. Statistical significance was defined as $P<0.05$; statistical high significance was defined as $P<0.01$. Error bars are given on the basis of calculated SD values.

Results

Encapsulation efficiency and drug loading efficiency

The liposomes were prepared using a modified ethanol injection method as shown in schematics in Figure 1A. The lipid and drug amounts along with drug loading efficiency (DLE) and encapsulation efficiency (EE) values for all liposomes including empty liposomes as well as both single drug-loaded and dual drug-loaded liposomes are consolidated in Table 1. For lipophilic drugs such as everolimus, the encapsulation efficiency was 99.1%±0.17% since they are water insoluble and as such incorporated almost completely in the liposome bilayer. For comparatively higher hydrophilic drug vinorelbine, the encapsulation efficiency was 23.6%±1%. The drug loading efficiency of everolimus in E-L and vinorelbine in V-L was 7.2%±0.01% and 3.4%±0.14%, respectively. Similarly, the EE of everolimus and vinorelbine in EV-L was 98.5%±1.2% and 24%±1.3%, respectively, while the DLE values were 7.29% ±0.1% and 3.5%±0.34%, respectively. Of note, the values did not change significantly in case of dual drug loading. Conceivably, everolimus and vinorelbine have completely separate spatial distribution inside the liposome and therefore do not compete for accommodation.

Table 1 Composition of liposomes, drug loading efficiency (DLE) and encapsulation efficiency (EE). Composition, drug loading efficiency and encapsulation efficiency of empty liposome (L), liposomes containing Everolimus (E-L), Vinorelbine (V-L), and combination of and combination of Everolimus and Vinorelbine (EV-L)

Liposome	DOPC (mg/mL)	Cholesterol (mg/mL)	DSPE(PEG)2000-OMe (mg/mL)	TTP (mg/mL)	E (mg/mL)	V (mg/mL)	DLE (%)	EE (%)
L	3.93	0.965	0.140	0.452	—	—	—	—
E-L	3.93	0.965	0.140	0.452	0.397±0.001	—	7.2±0.01	99.1±0.17
V-L	3.93	0.965	0.140	0.452	—	0.189±0.008	3.4±0.14	23.6±1
EV-L	3.93	0.965	0.140	0.452	0.394±0.005	0.192±0.01	7.29±0.1(E), 3.5±0.34 (V)	98.5±1.2 (E), 24±1.3 (V)

Abbreviations: DOPC, 1,2-dioleoyl-sn-glycero-3-phosphocholine; DSPE-PEG2000-OMe, 1,2-distearoyl-sn-glycero-3-phosphoethanolamine-N-[methoxy(polyethylene glycol)-2000] (ammonium salt); TTP, tumor targeting peptide; E, Everolimus; V, Vinorelbine; DLE, drug loading efficiency; EE, encapsulation efficiency.

Characterization of liposomes

The physicochemical characteristics of empty liposome (L) along with liposome containing Everolimus (E-L), Vinorelbine (V-L) and a combination of both (EV-L) were consolidated in Table 2. The entrapment of drugs caused mostly minor changes in the size and PDI of the liposomes except for encapsulation of Everolimus (E-L) where the PDI of the liposomes increased significantly. On the contrary, encapsulation of Vinorelbine (V-L) or a combination of everolimus and vinorelbine (EV-L) did not affect the PDI much. Everolimus is water insoluble, so it is entrapped in the liposome bilayer. This results in significant change in the bilayer properties causing higher variability in liposome size distribution that is reflected by an increased polydispersity index. In contrast, Vinorelbine, being highly water soluble, is entrapped in the aqueous core of the liposome, thereby not exerting any significant effect on the liposome bilayer. The hydrodynamic size distribution histograms and TEM images of the liposomes are shown in Figure 1B and C, respectively. As expected, the liposomes in the TEM images appeared slightly smaller than DLS measurements, which is consistent with previously published literature.[47] However, the zeta potentials were significantly different among the liposomes. The empty liposomes had a zeta potential of 23.1±0.26 mV. Encapsulation of Everolimus decreased the zeta potential to 12.5±0.79 mV, whereas encapsulation of Vinorelbine increased it to 35.26±1.5 mV. The liposomes encapsulating both the drugs had more or less similar zeta potential (26.6 ±1.4 mV) compared to the empty liposomes.

In vitro cellular uptake of liposomes in RCC cell lines

We then sought to analyze the in vitro cellular uptake of Rhodamine-PE-labeled liposomes. As can be seen from Figure 2, after 4 hrs treatment, cellular uptake of the TTP-conjugated liposomes (TL) was considerably higher in both 786-O and A498 RCC cell lines than that of control liposome (CL) prepared using same ratio of lipids except TTP-conjugated lipopeptide. This demonstrates the excellent targeting efficiency of TTP-conjugated liposomal formulation.

Table 2 Characterization of liposomal drug formulations. Hydrodynamic size, polydispersity index (PDI) and zeta potential of empty liposomes (L), or liposomes containing Everolimus (E-L), Vinorelbine (V-L), and combination of Everolimus and Vinorelbine (EV-L). All the measurements were performed in deionized water at 25°C

Liposome	Size (nm)	PDI	Zeta (mV)
L	72.73±1.13	0.178±0.01	23.1±0.26
E-L	70.16±0.48	0.244±0.005	12.5±0.79
V-L	60.91±0.28	0.160±0.006	35.26±1.5
EV-L	65.95±0.63	0.198±0.013	26.6±1.4

Abbreviations: PDI, polydispersity index.

In vivo biodistribution of liposomes in RCC xenograft-bearing mice

We also analyzed the in vivo biodistribution of the liposomes in RCC tumor-bearing mice. For this experiment, we developed subcutaneous 786-O or A498 tumors in male SCID mice and injected IR-780-dye labeled liposomes via intravenous route. We used IR-780-dye in this experiment since it absorbs and emits in IR region of the spectrum that is less absorbed by living tissue. There is no autofluorescence interfering with the signal intensity from mice fur in this region as well. As demonstrated in Figure 3A-B, TL showed higher tumor-specific signal compared to CL in both 786-O and A498 xenografts at 24 hrs and 48 hrs after administration. The ex vivo imaging of the tumors and major organs corroborate with in vivo imaging (Figure 3C and D). Interestingly, lungs from mice treated with CL showed stronger signal compared to the lungs of TL treated mice. This suggests that the addition of TTP helped to reduce nonspecific accumulation of the liposomes in the lungs.

In vitro efficacy of drug-loaded liposomes in RCC

Since TL showed significantly higher in vitro cellular uptake and in vivo tumor targeting compared to CL, we used TL for all further efficacy studies. We tested the drug-loaded liposomal formulations for their efficacy in reducing in vitro cell viability in 786-O and A498 cells. The results are consolidated in Figure 4. The dual drug-loaded liposomes had better efficacy in both 786-O (Figure 4A) and A498 (Figure 4B) cell line. However, the difference was not so prominent between V-L and EV-L in both the cell lines. Nonetheless, the above experiments demonstrated that dual drug-loaded liposomes were efficient in decreasing cell viability.

In vivo efficacy of drug-loaded liposomes in RCC xenografts

We then utilized a recently popular concept of single mouse trial to analyze the efficacy of the drug-loaded liposomes. This approach has been well accepted for PDX models by various research groups as well as Charles River Laboratories.[40–46]

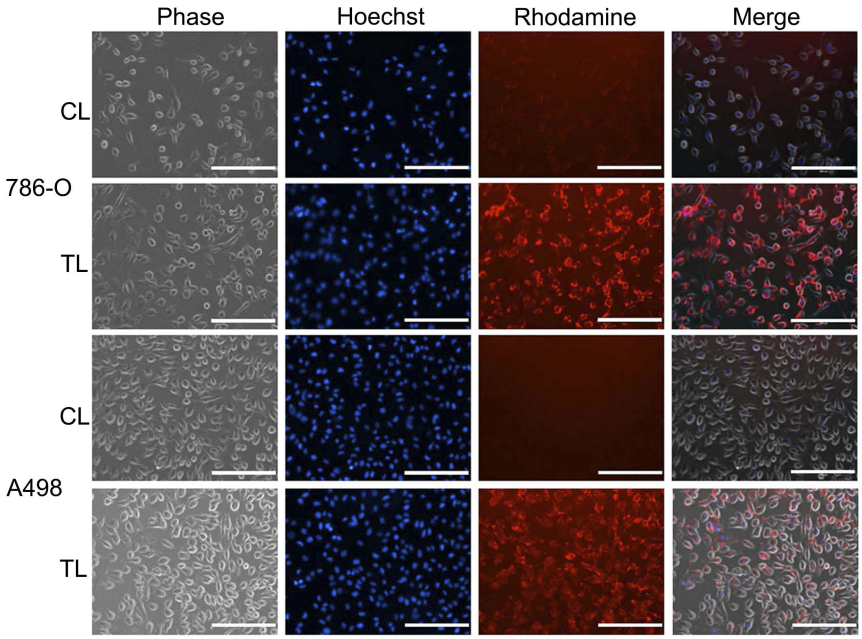

Figure 2 In vitro cellular uptake of Rhodamine-PE-labeled liposomes in RCC cell lines. 786-O and A498 cells were treated with Rhodamine-PE-labeled control liposomes (CL) or TTP-conjugated Liposomes (TL) for 4 hrs. Nuclei of the cells were counterstained with Hoechst for the last 30 mins. Finally, cells were washed three times with PBS and images were captured using EVOS fluorescence microscope under bright field, blue and red channel. TL treated cells showed significantly higher uptake of Rhodamine dye compared to CL-treated cells in all cell lines. Bar length =200 µm.
Abbreviations: CL, control liposome; TL, tumor targeting peptide-conjugated liposome.

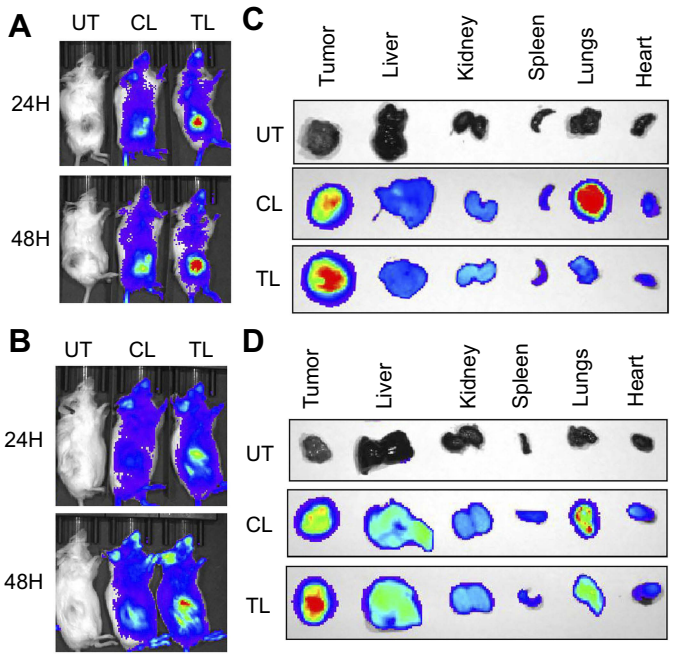

Figure 3 In vivo biodistribution of IR-780-dye-labeled liposomes in RCC xenografts. IVIS imaging showing higher tumor accumulation of IR-780 dye-labeled TTP-conjugated liposomes (TL) compared to control liposomes (CL) at 24 hrs (upper panel) and 48 hrs (lower panel) after IV administration into mice bearing subcutaneous 786-O (**A**) and A498 tumors (**B**) One untreated mouse (UT) was used for background correction. Ex vivo imaging of 786-O (**C**) and A498 (**D**) tumors and major organs, respectively, harvested at 48 hrs demonstrated significant higher tumor uptake of TL compared to CL. Interestingly, significantly higher lung accumulation of CL was observed compared to TL.
Abbreviations: UT, untreated; CL, control liposome; TL, tumor targeting peptide-conjugated liposome.

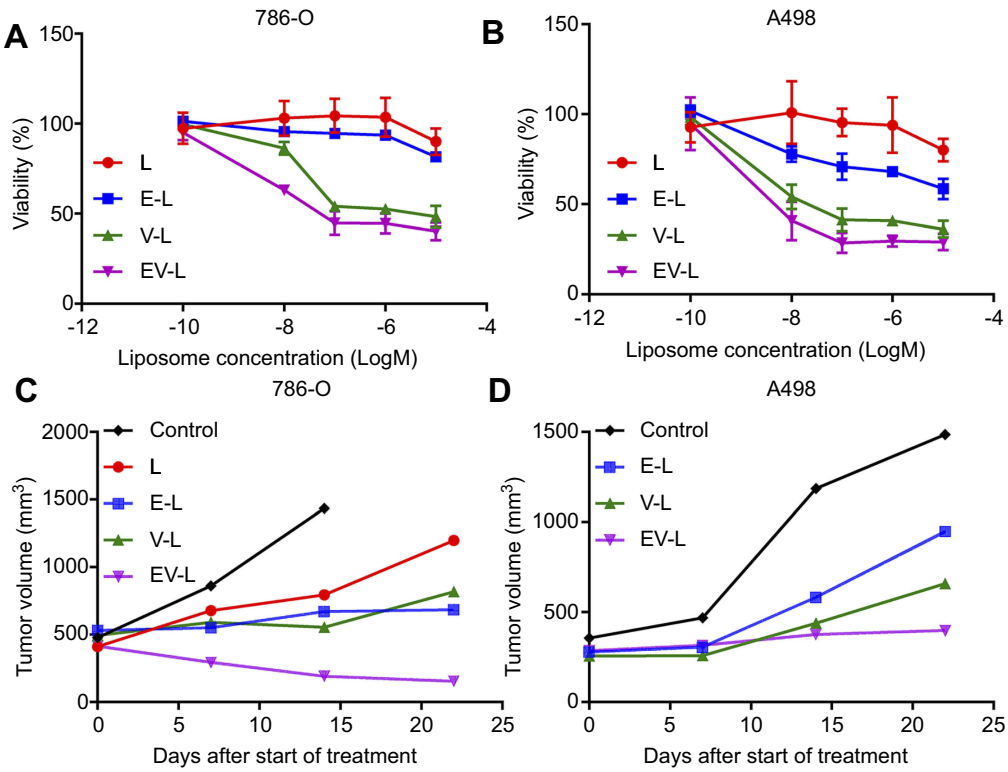

Figure 4 In vitro and in vivo efficacy of drug-loaded liposomes in RCC cell lines. 786-O (**A**) and A498 (**B**) cells were treated with various drug-loaded TTP-conjugated Liposomes for 72 hrs. Then, cell viability was determined with MTS assay. Dual drug-loaded liposomes showed higher reduction in cell viability compared to single drug-loaded liposomes in all cell lines. (**C**) 5×10^6 786-O cells were subcutaneously injected into the right flanks of 8 weeks old male SCID mice. Tumors were allowed to grow until the average tumor size is ~400–500 mm^3. Then, mice were treated with drug-loaded liposomes (one mouse per treatment group) 3x/wk for 3 weeks. Tumors were measured weekly and tumor volume is plotted to obtain the respective growth curves. In both cases, dual-drug-loaded liposomes demonstrated significant inhibition compared to single drug-loaded liposomes. Some of the mice were sacrificed before the completion of experiment due to ulceration of tumors. (**D**) Similar results were obtained in A498 xenografts.

This approach employs a single mouse per treatment arm, thus reducing the cost of animal experiments. By measuring longitudinal growth of the tumors, the most effective treatment can be reliably identified in a cost-effective manner. We also started the treatment when the tumors became 300–500 mm^3 which is significantly higher than 50–100 mm^3 volumes described in majority of published literature. As can be seen from Figure 4C, not only EV-L was better than the single drug-loaded liposomes, but also are capable of actually decreasing the tumor volume from the starting volume in 786-O xenografts. Similar experiments in A498 xenografts also identified EV-L as the most potent formulation among the treatment groups (Figure 4D). The H&E and Ki67 staining of the tumor sections obtained from 786-O and A498 xenografts (Figure 5A–C) demonstrates the significantly higher antiproliferative activity of EV-L in both tumor tissues. Major organs such as liver, kidney and spleen are not adversely affected by the drug-loaded liposome treatment as evident from no significant change in gross morphology (Figures S1 and S2).

In order to confirm whether these observations are reproducible, we selected the formulation EV-L for further validation studies in cohorts of 5 mice (Figure 6A–D). We obtained more or less similar results with the single mouse trials. This demonstrates the usefulness of the single mouse trial in identifying the best treatment strategy of combating cancer.

Inhibition of lung metastases

RCC tumors are well known for their high levels of lung metastases.[48] We sought to determine whether our drug-loaded liposomal formulations are capable of reducing the lung metastases. The H&E staining of the lung sections from the experimental mice showed a large number of metastatic nodules in the untreated mouse or mice treated with liposome only (L) or liposomes loaded with everolimus (E-L) or vinorelbine (V-L). In contrast, EV-L showed only a few nodules (Figure 7). Similar result was observed in the validation study as well (data not shown). These results demonstrated that EV-L was capable of reducing the lung metastases of RCC tumors.

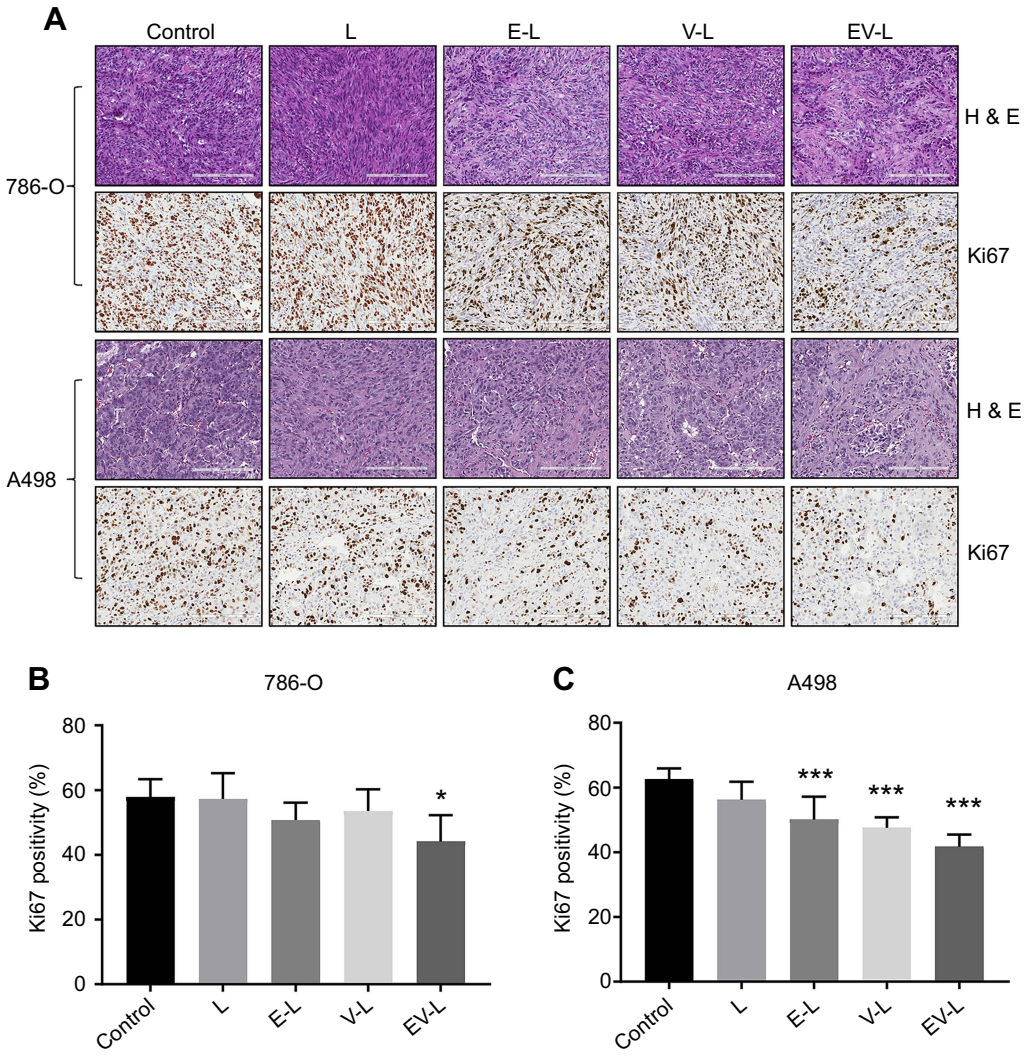

Figure 5 H&E and Ki67 staining of tumor sections obtained from the single mouse trial. (**A**) Representative images of the H&E and Ki67-stained tumor sections from different treatment groups displayed comparatively higher anti-proliferative activity of EV-L. Bar length =200 μm. (**B & C**) Quantification of Ki67 positive nuclei in 786-O and A498 tumor sections, respectively. * and *** denotes $p<0.05$ and $p<0.001$ compared to control, respectively.
Abbreviation: H & E, hematoxylin and eosin.

Discussion

RCC is the most prevalent form of kidney cancer and is accountable for about 90% of all kidney cancer incidences.[2] Although early stage RCC patients are likely to have a better prognosis, advanced RCC is a lethal disease with a 5 years survival rate of 11.7% only.[49] Metastatic progression along with acquired resistance towards chemotherapy and radiotherapy are responsible for this dismal 5 years survival rate. Metastatic progression is detected at clinical presentation in about one-third of RCC patients while development of distant metastases after resection of primary tumor was seen in up to 50% patients.[50] Therefore, novel treatment strategies that can impede the primary tumor growth as well as the metastatic progression represent an unmet clinical need.

Everolimus (RAD-001, Afinitor®) is an orally bioavailable inhibitor of the mammalian target of rapamycin (mTOR), a protein kinase and key regulator of metabolic homeostasis, that is implicated in a number of diseases including RCC.[51] Treatment with everolimus led to the inhibition of cell growth, migration and invasion in various RCC cell lines in vitro.[52,53] Everolimus has been shown to possess anti-angiogenic properties as well, though its mode of action is different from other vascular endothelial growth factor receptor (VEGFR)-tyrosin kinase inhibitors.[38] Several studies demonstrated that everolimus inhibits the expression of VEGF in tumor cells.[52,54] Everolimus is now approved for second- and third-line therapy in patients with advanced RCC, but it did not

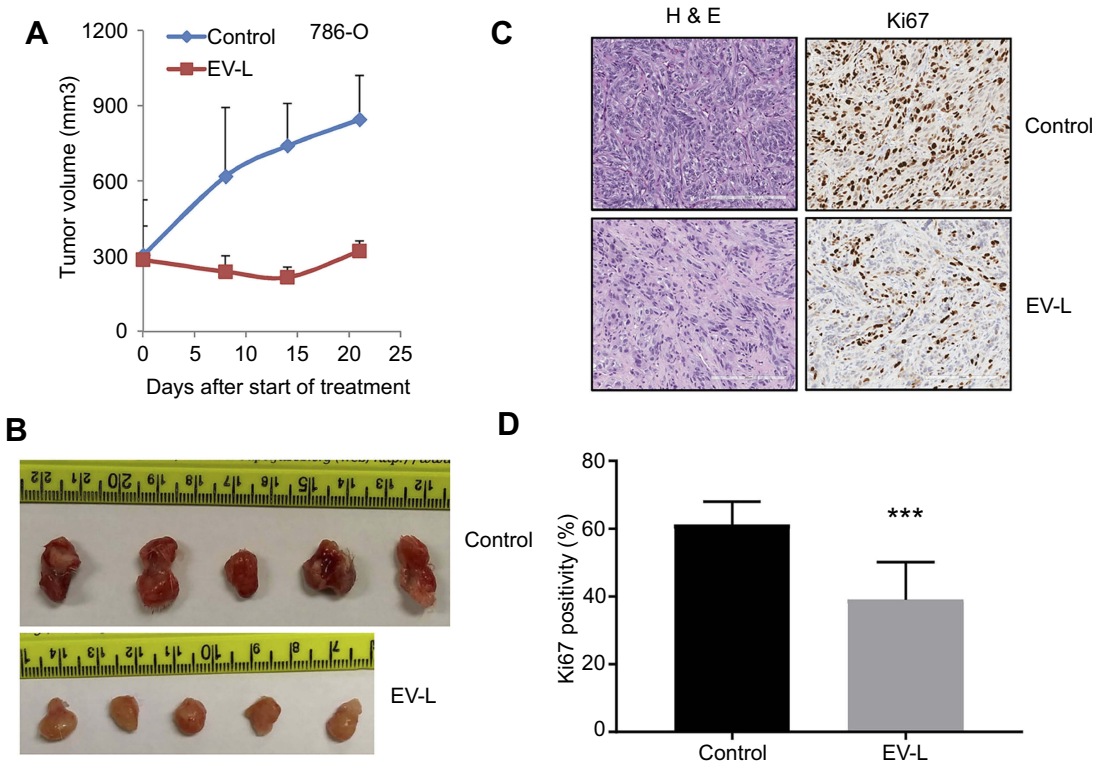

Figure 6 Validation of the result obtained from single mouse trial in cohorts of 5 mice. (**A**) 5×10^6 786-O cells were subcutaneously injected into the right flanks of 8 weeks old male SCID mice. Tumors were allowed to grow until the average tumor size is ~300 mm^3. Then, mice were treated with vehicle or EV-L (five mice per treatment group) 3x/wk for 3 weeks. Tumors were measured weekly and tumor volume is plotted to obtain the respective growth curves. EV-L demonstrated significant inhibition compared to the vehicle group. (**B**) Images of the harvested tumors at the end of the experiment. (**C**) Representative images of H&E and Ki67 staining of the tumor tissue sections. Bar length =200 μm. (**D**) Quantification of Ki67 positive nuclei. *** denotes $p<0.001$ compared to control.
Abbreviation: H & E, hematoxylin and eosin.

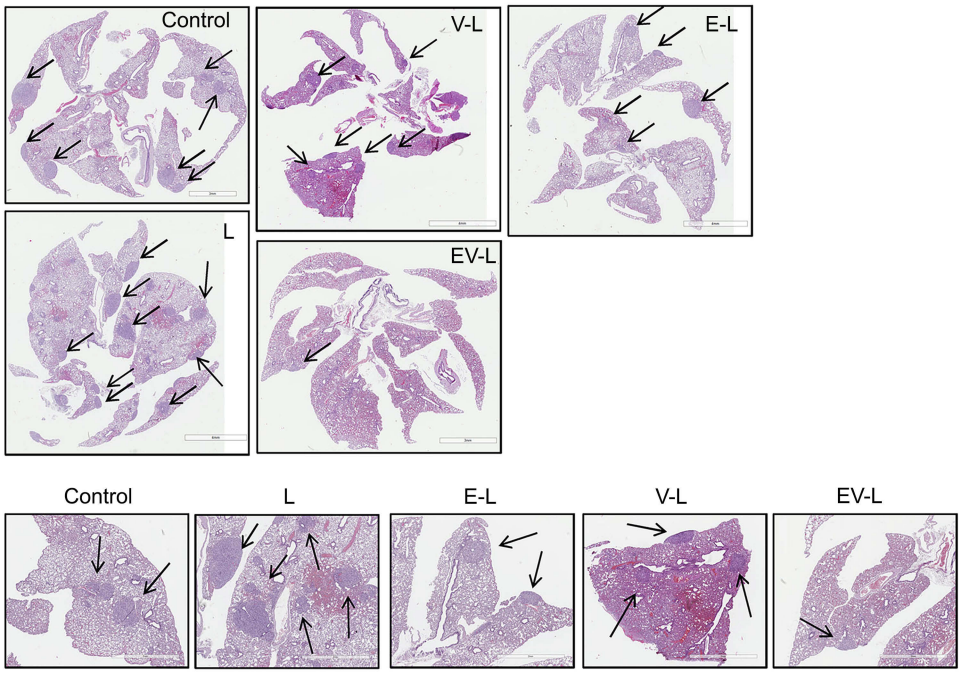

Figure 7 Inhibition of lung metastasis in 786-O xenografted mice. The dual drug-loaded liposomes significantly inhibited lung metastasis in mice bearing 786-O subcutaneous tumors compared to untreated, liposome only of single drug-loaded liposomes. Metastatic nodules were indicated by black arrows. The lower panel demonstrates magnified portions from the upper panel.

offer any significant clinical benefit in first-line setting even in combination with bevacizumab.[55] A recent Phase II study demonstrated a significant increase in progression-free survival and overall survival in second-line combination treatment with everolimus plus lenvatinib (a novel TKI) compared to the single-agent everolimus.[23] The safety profile of everolimus is deemed as favorable and no substantial impact on the quality of life of everolimus-treated patients has been observed. Even so, most common side effects of everolimus include nausea, anorexia, diarrhea, stomatitis, pneumonitis and rash.[56]

Vinorelbine is one of the vinca alkaloids that are being used as anticancer agents in various combination chemotherapy regimens. Vinca alkaloids induce metaphase arrest via disrupting the microtubules of the mitotic spindle apparatus.[57] Among them, vinblastine, vincristine, vindesine and vinflunine have been tested in several clinical trials including patients with advanced RCC, either as a monotherapy or in combination with other drugs.[57–59] In the United States, vinorelbine has been approved as a first-line therapy for patients with advanced non-small cell lung cancer (NSCLC).[60] Additionally, it was effective in impeding metastasis in advanced stage breast cancer patients.[60] A combination of vinorelbine and trastuzumab was shown to be significantly more effective for the treatment of metastatic breast cancer compared to the monotherapy.[61] Nonetheless, vinorelbine has been shown to have some side effects including neutropenia, peripheral neuropathy and gastrointestinal (GI) complications.[60]

Despite its effectiveness in several cancers, there are not many studies analyzing the efficacy of vinorelbine in RCC. A previous study from our group demonstrated that vinorelbine in combination with anti-angiogenic therapy strongly inhibits primary RCC tumor growth in vivo.[36] This study, combined with the fact that everolimus is known for its anti-angiogenic activity, inspired us to test the efficacy of a liposomal combination of everolimus and vinorelbine in RCC xenografts. Towards this end, we developed a tumor-targeted PEGylated liposomal formulation (TL) by decorating its surface with a proprietary tumor-targeting peptide (TTP). We observed significantly higher tumor-targeting efficacy of TL compared to the non-targeting control (CL) in two different RCC xenografts. Consequently, we selected TL for drug loading and efficacy experiments.

Notably, the average hydrodynamic diameters of the empty liposomes as well as all the drug-loaded liposomes were below 100 nm potentiating better penetration through the blood-tumor barriers and tumor microenvironment.[62] Similarly, the zeta potentials for all the liposomes were positive suggesting stronger interactions with negatively charged cell membranes.[63] Zeta potential is also a measure of the electrostatic repulsion or attraction between particles in a colloidal suspension and usually predicts the stability of the suspension.[63] A higher value of zeta potential, whether positive or negative, typically indicates better stability. L, V-L and EV-L had zeta potential values of 23.1 ±0.26 mV, 35.26±1.5 mV and 26.6±1.4 mV, respectively, suggesting stable formulations. Only E-L had a lower zeta potential of 12.5±0.79 mV, indicating somewhat lower stability of E-L. Interestingly, V-L and EV-L had higher zeta potential values than L and E-L, respectively. We believe that this increase is presumably caused by the attachment of some vinorelbine molecules to the liposome surface through electrostatic interaction even if most of the vinorelbine was encapsulated in the aqueous core of the liposomes for its hydrophilic nature.

Nonetheless, we hypothesized that our tumor-targeted liposomal formulation will enable us to use lower doses of everolimus and vinorelbine and still be effective. This will also be helpful in reducing the side effects of those drugs. Therefore, in our study, we have used nominal doses of everolimus (1 mg/kg, 3x/week) and vinorelbine (0.475 mg/kg, 3x/week) for the treatment of mice with RCC. Notably, we achieved remarkable tumor inhibition while using lower doses of these drugs than are usually administered. For instance, everolimus is typically administered daily via oral route at 1–5 mg/kg/day.[64] Similarly the usual dose of vinorelbine is 4.8–5 mg/kg/week via intravenous or intraperitoneal route.[36,65] We also started the treatment with a larger initial tumor size than are reported in a majority of reported animal studies and still observed significant inhibition in tumor growth. Most importantly, we were able to inhibit the metastatic progression which is primarily responsible for the poor survival in patients with advanced RCC.

Conclusion

To summarize, we have developed a novel tumor-targeted liposomal formulation and demonstrated its targeting efficacy in two different RCC xenografts. We further demonstrated that the same formulation, when loaded with everolimus and vinorelbine, was successful in inhibiting proliferation in vitro and tumor growth and lung metastasis in vivo in those two RCC cell lines. Taken together, our work demonstrates that a tumor-targeted liposomal formulation encapsulating everolimus and vinorelbine could be

a promising approach for the treatment of metastatic RCC where there is a clear unmet need for effective therapies.

Acknowledgments

This work was supported by National Institue of Health (NIH) grants CA78383 and CA150190 and Florida Department of Health Cancer Research Chair Fund Florida #3J (DM). The authors would like to thank Brandy Edenfield for immunohistochemistry and Laura Lewis-Tuffin for assistance with digitization of the slides. The authors would also like to thank the Mayo Microscopy and Cell Analysis Core for experimental and technical support.

Disclosure

DM has applied for protection of intellectual property related to the results in the manuscript. KP, VSM, and DM report a patent 2018-301 pending. The authors report no other conflicts of interest in this work.

References

1. Siegel RL, Miller KD, Jemal A. Cancer statistics, 2018. *CA Cancer J Clin*. 2018;68(1):7–30. doi:10.3322/caac.21442
2. Low G, Huang G, Fu W, Moloo Z, Girgis S. Review of renal cell carcinoma and its common subtypes in radiology. *World J Radiol*. 2016;8(5):484–500. doi:10.4329/wjr.v8.i5.484
3. Shuch B, Amin A, Armstrong AJ, et al. Understanding pathologic variants of renal cell carcinoma: distilling therapeutic opportunities from biologic complexity. *Eur Urol*. 2015;67(1):85–97. doi:10.1016/j.eururo.2014.04.029
4. Goyal R, Gersbach E, Yang XJ, Rohan SM. Differential diagnosis of renal tumors with clear cytoplasm: clinical relevance of renal tumor subclassification in the era of targeted therapies and personalized medicine. *Arch Pathol Lab Med*. 2013;137(4):467–480. doi:10.5858/arpa.2012-0085-RA
5. Woldemeskel M. Renal cell carcinoma in humans and animals: a brief literature review. *J Clin Exp Pathol*. 2013;3(2). doi:10.4172/2161-0681.S7-001
6. Bukowski RM. Cytokine therapy for metastatic renal cell carcinoma. *Semin Urol Oncol*. 2001;19(2):148–154.
7. Santoni M, Massari F, Di Nunno V, et al. Immunotherapy in renal cell carcinoma: latest evidence and clinical implications. *Drugs Context*. 2018;7:212528.
8. Heng DY. The next 10 years: challenges for the future and overcoming resistance to targeted therapies for renal cell carcinoma. *Can Urol Assoc J*. 2016;10(11–12Suppl7):S256–S258.
9. Gore ME, Larkin JM. Challenges and opportunities for converting renal cell carcinoma into a chronic disease with targeted therapies. *Br J Cancer*. 2011;104(3):399–406.
10. Cho DC. Therapeutic challenges in advanced renal cell carcinoma. *Clin Pract (Lond)*. 2013;10(1):39–46. doi:10.2217/cpr.12.77
11. Bayat Mokhtari R, Homayouni TS, Baluch N, et al. Combination therapy in combating cancer. *Oncotarget*. 2017;8(23):38022–38043. doi:10.18632/oncotarget.16723
12. Yap TA, Omlin A, de Bono JS. Development of therapeutic combinations targeting major cancer signaling pathways. *J Clin Oncol*. 2013;31(12):1592–1605. doi:10.1200/JCO.2011.37.6418
13. Albain KS, Nag SM, Calderillo-Ruiz G, et al. Gemcitabine plus paclitaxel versus paclitaxel monotherapy in patients with metastatic breast cancer and prior anthracycline treatment. *J Clin Oncol*. 2008;26(24):3950–3957. doi:10.1200/JCO.2007.11.9362
14. Procopio G, Ratta R, de Braud F, Verzoni E. Combination therapies for patients with metastatic renal cell carcinoma. *Lancet Oncol*. 2018;19(3):281–283. doi:10.1016/S1470-2045(18)30092-5
15. Buonerba C, Di Lorenzo G, Sonpavde G. Combination therapy for metastatic renal cell carcinoma. *Ann Transl Med*. 2016;4(5):100. doi:10.21037/atm.2016.04.05
16. Stephan S, Datta K, Wang E, et al. Effect of rapamycin alone and in combination with antiangiogenesis therapy in an orthotopic model of human pancreatic cancer. *Clin Cancer Res*. 2004;10(20):6993–7000. doi:10.1158/1078-0432.CCR-04-0808
17. Larkin J, Esser N, Calvo E, et al. Efficacy of sequential treatment with sunitinib-everolimus in an orthotopic mouse model of renal cell carcinoma. *Anticancer Res*. 2012;32(7):2399–2406.
18. Rini BI, Bellmunt J, Clancy J, et al. Randomized phase III trial of temsirolimus and bevacizumab versus interferon alfa and bevacizumab in metastatic renal cell carcinoma: INTORACT trial. *J Clin Oncol*. 2014;32(8):752–759. doi:10.1200/JCO.2013.50.5305
19. Ravaud A, Barrios CH, Alekseev B, et al. RECORD-2: phase II randomized study of everolimus and bevacizumab versus interferon α-2a and bevacizumab as first-line therapy in patients with metastatic renal cell carcinoma. *Ann Oncol*. 2015;26(7):1378–1384. doi:10.1093/annonc/mdv170
20. Flaherty KT, Manola JB, Pins M, et al. Best: a randomized phase ii study of vascular endothelial growth factor, RAF kinase, and mammalian target of rapamycin combination targeted therapy with bevacizumab, sorafenib, and temsirolimus in advanced renal cell carcinoma—a trial of the ECOG–ACRIN cancer research group (E2804). *J Clin Oncol*. 2015;33(21):2384–2391. doi:10.1200/JCO.2015.60.9727
21. Molina AM, Feldman DR, Voss MH, et al. Phase 1 trial of everolimus plus sunitinib in patients with metastatic renal cell carcinoma. *Cancer*. 2012;118(7):1868–1876. doi:10.1002/cncr.26429
22. Patel PH, Senico PL, Curiel RE, Motzer RJ. Phase I study combining treatment with temsirolimus and sunitinib malate in patients with advanced renal cell carcinoma. *Clin Genitourin Cancer*. 2009;7(1):24–27. doi:10.3816/CGC.2009.n.004
23. Motzer RJ, Hutson TE, Glen H, et al. Lenvatinib, everolimus, and the combination in patients with metastatic renal cell carcinoma: a randomised, phase 2, open-label, multicentre trial. *Lancet Oncol*. 2015;16(15):1473–1482. doi:10.1016/S1470-2045(15)00290-9
24. Rini BI, Halabi S, Rosenberg JE, et al. Phase III trial of bevacizumab plus interferon alfa versus interferon alfa monotherapy in patients with metastatic renal cell carcinoma: final results of CALGB 90206. *J Clin Oncol*. 2010;28(13):2137–2143. doi:10.1200/JCO.2009.26.5561
25. Motzer RJ, Tannir NM, McDermott DF, et al. Nivolumab plus ipilimumab versus sunitinib in advanced renal-cell carcinoma. *N Eng J Med*. 2018;378(14):1277–1290. doi:10.1056/NEJMoa1712126
26. Motzer RJ, Penkov K, Haanen J, et al. Avelumab plus axitinib versus sunitinib for advanced renal-cell carcinoma. *N Eng J Med*. 2019;380(12):1103–1115. doi:10.1056/NEJMoa1816047
27. Rini BI, Plimack ER, Stus V, et al. Pembrolizumab plus axitinib versus sunitinib for advanced renal-cell carcinoma. *N Eng J Med*. 2019;380(12):1116–1127. doi:10.1056/NEJMoa1816714
28. Lopez JS, Banerji U. Combine and conquer: challenges for targeted therapy combinations in early phase trials. *Nat Rev Clin Oncol*. 2017;14(1):57–66. doi:10.1038/nrclinonc.2016.96
29. Sercombe L, Veerati T, Moheimani F, Wu SY, Sood AK, Hua S. Advances and challenges of liposome assisted drug delivery. *Front Pharmacol*. 2015;6:286. doi:10.3389/fphar.2015.00286

30. Ulrich AS. Biophysical aspects of using liposomes as delivery vehicles. *Biosci Rep*. 2002;22(2):129–150.
31. Immordino ML, Dosio F, Cattel L. Stealth liposomes: review of the basic science, rationale, and clinical applications, existing and potential. *Int J Nanomedicine*. 2006;1(3):297–315.
32. Jain A. Jain. Advances in Tumor Targeted Liposomes. *Curr Mol Med*. 2018;18(1):44–57. doi:10.2174/1566524018666180416101522
33. Dong M, Luo L, Ying X, et al. Comparable efficacy and less toxicity of pegylated liposomal doxorubicin versus epirubicin for neoadjuvant chemotherapy of breast cancer: a case-control study. *Onco Targets Ther*. 2018;11:4247–4252. doi:10.2147/OTT.S162003
34. Deshpande PP, Biswas S, Torchilin VP. Current trends in the use of liposomes for tumor targeting. *Nanomedicine (Lond)*. 2013;8 (9):1509–1528. doi:10.2217/nnm.13.118
35. Bulbake U, Doppalapudi S, Kommineni N, Khan W. Liposomal formulations in clinical use: an updated review. *Pharmaceutics*. 2017;9(4):12. doi:10.3390/pharmaceutics9020012
36. Sinha S, Cao Y, Dutta S, Wang E, Mukhopadhyay D. VEGF neutralizing antibody increases the therapeutic efficacy of vinorelbine for renal cell carcinoma. *J Cell Mol Med*. 2010;14(3):647–658. doi:10.1111/j.1582-4934.2008.00578.x
37. Piguet A-C, Majumder S, Maheshwari U, et al. Everolimus is a potent inhibitor of activated hepatic stellate cell functionsin vitroandin vivo, while demonstrating anti-angiogenic activities. *Clin Sci*. 2014;126(11):775–791. doi:10.1042/CS20130081
38. Lane HA, Wood JM, McSheehy PM, et al. mTOR inhibitor RAD001 (everolimus) has antiangiogenic/vascular properties distinct from a VEGFR tyrosine kinase inhibitor. *Clin Cancer Res*. 2009;15 (5):1612–1622. doi:10.1158/1078-0432.CCR-08-2057
39. Jaafar-Maalej C, Diab R, Andrieu V, Elaissari A, Fessi H. Ethanol injection method for hydrophilic and lipophilic drug-loaded liposome preparation. *J Liposome Res*. 2009;20(3):228–243. doi:10.3109/08982100903347923
40. Bug D, Oswald E, Grote A, et al. Abstract 4815: humanized single mouse trial: a preclinical platform feasible for immune-oncology drug screening and translational biomarker development. *Cancer Res*. 2017;77(13 Supplement):4815.
41. Gredy C, Schüler JB, Zanella N, Fiebig -H-H, Metz T. Abstract 2890: single mouse trials, a concept using patient-derived tumor xenografts for large scale in vivo screens. *Cancer Res*. 2015;75(15 Supplement):2890.
42. Knudsen ES, Balaji U, Mannakee B, et al. Pancreatic cancer cell lines as patient-derived avatars: genetic characterisation and functional utility. *Gut*. 2017.
43. Malaney P, Nicosia SV, Dave V. One mouse, one patient paradigm: new avatars of personalized cancer therapy. *Cancer Lett*. 2014;344 (1):1–12. doi:10.1016/j.canlet.2013.10.010
44. Mignard C, Boisferon MHD, Bichat F, France D, Duchamp O. Abstract 2170: single mouse preclinical trial: a tool for translational research. *Cancer Res*. 2018;78(13 Supplement):2170.
45. Murphy B, Yin H, Maris JM, et al. Evaluation of alternative in vivo drug screening methodology: a single mouse analysis. *Cancer Res*. 2016;76(19):5798–5809. doi:10.1158/0008-5472.CAN-16-0122
46. Suarez C, Martinez M, Trilla E, et al. Patient-derived AVATAR mouse models to predict prognosis in advanced renal cell carcinoma. *J Clin Oncol*. 2016;34(2_suppl):551. doi:10.1200/jco.2016.34.2_suppl.551
47. Souza TGF, Ciminelli VST, Mohallem NDS. A comparison of TEM and DLS methods to characterize size distribution of ceramic nanoparticles. *J Phys*. 2016;733:012039.
48. Bianchi M, Sun M, Jeldres C, et al. Distribution of metastatic sites in renal cell carcinoma: a population-based analysis. *Ann Oncol*. 2012;23(4):973–980. doi:10.1093/annonc/mdr362
49. Siegel RL, Miller KD, Jemal A. Cancer statistics, 2017. *CA Cancer J Clin*. 2017;67(1):7–30. doi:10.3322/caac.21387
50. Bukowski RM. Natural history and therapy of metastatic renal cell carcinoma: the role of interleukin-2. *Cancer*. 1997;80(7):1198–1220.
51. Hanna SC, Heathcote SA, Kim WY. mTOR pathway in renal cell carcinoma. *Expert Rev Anticancer Ther*. 2008;8(2):283–292. doi:10.1586/14737140.8.2.283
52. Rosa R, Damiano V, Nappi L, et al. Angiogenic and signalling proteins correlate with sensitivity to sequential treatment in renal cell cancer. *Br J Cancer*. 2013;109(3):686–693. doi:10.1038/bjc.2013.360
53. Wu SW, Chen PN, Lin CY, Hsieh YS, Chang HR. Everolimus suppresses invasion and migration of renal cell carcinoma by inhibiting FAK activity and reversing epithelial to mesenchymal transition in vitro and in vivo. *Environ Toxicol*. 2017;32(7):1888–1898. doi:10.1002/tox.22411
54. Alshaker H, Wang Q, Böhler T, et al. Combination of RAD001 (everolimus) and docetaxel reduces prostate and breast cancer cell VEGF production and tumour vascularisation independently of sphingosine-kinase-1. *Sci Rep*. 2017;7(1):3493. doi:10.1038/s41598-017-03728-3
55. Buti S, Leonetti A, Dallatomasina A, Bersanelli M. Everolimus in the management of metastatic renal cell carcinoma: an evidence-based review of its place in therapy. *Core Evid*. 2016;11:23–36. doi:10.2147/CE.S98687
56. Houghton PJ. Everolimus. *Clin Cancer Res*. 2010;16(5):1368–1372. doi:10.1158/1078-0432.CCR-09-1314
57. Moudi M, Go R, Yien CY, Nazre M. Vinca alkaloids. *Int J Prev Med*. 2013;4(11):1231–1235.
58. El-Galley R, Keane TE, Sun C. Camptothecin analogues and vinblastine in the treatment of renal cell carcinoma: an in vivo study using a human orthotopic renal cancer xenograft. *Urol Oncol*. 2003;21 (1):49–57.
59. Goldstein D, Ackland SP, Bell DR, et al. Phase II study of vinflunine in patients with metastatic renal cell carcinoma. *Invest New Drugs*. 2006;24(5):429–434.
60. Gregory RK, Smith IE. Vinorelbine–a clinical review. *Br J Cancer*. 2000;82(12):1907–1913.
61. Stravodimou A, Zaman K, Voutsadakis IA. Vinorelbine with or without trastuzumab in metastatic breast cancer: a retrospective single institution series. *ISRN Oncol*. 2014;2014:289836.
62. Blanco E, Shen H, Ferrari M. Principles of nanoparticle design for overcoming biological barriers to drug delivery. *Nat Biotechnol*. 2015;33(9):941–951.
63. Honary S, Zahir F. Effect of zeta potential on the properties of nano-drug delivery systems - a review (part 1). *Trop J Pharm Res*. 2013;12(2):255–264.
64. O'Reilly T, McSheehy PM, Wartmann M, Lassota P, Brandt R, Lane HA. Evaluation of the mTOR inhibitor, everolimus, in combination with cytotoxic antitumor agents using human tumor models in vitro and in vivo. *Anticancer Drugs*. 2011;22(1):58–78.
65. Tsuruo T, Inaba M, Tashiro T, et al. Evaluation of antitumor activity of navelbine (vinorelbine ditartrate) against human breast carcinoma xenografts based on its pharmacokinetics in nude mice. *Anticancer Drugs*. 1994;5(6):634–640.

Supplementary material

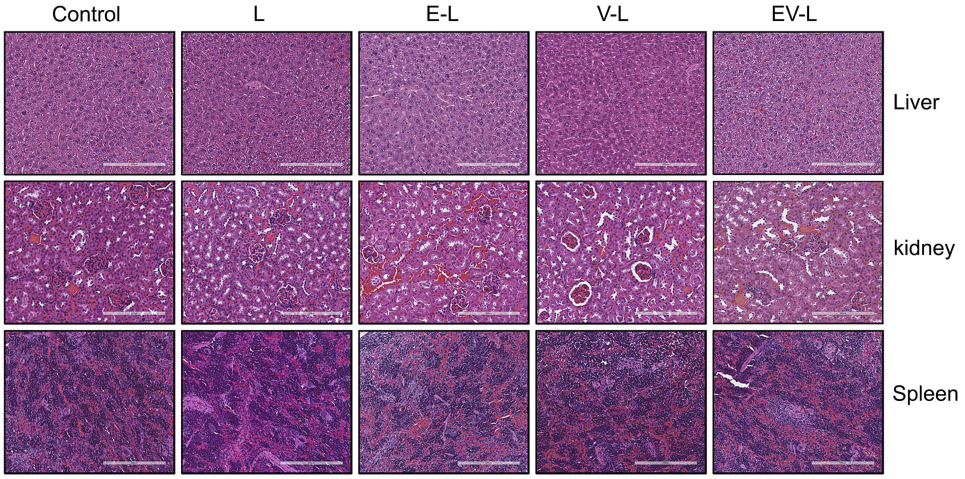

Figure S1 H&E staining of liver, kidney and spleen collected from mice bearing 786-O xenografts. Bar length =200 μm.

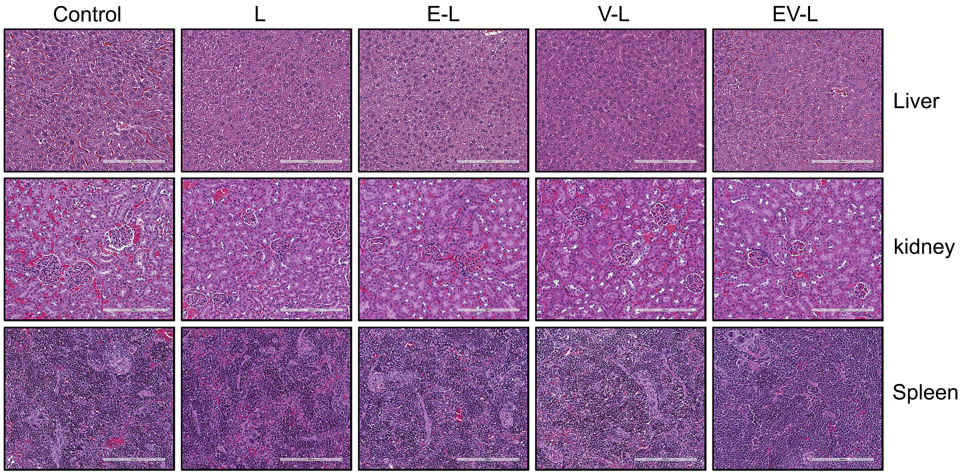

Figure S2 H&E staining of liver, kidney and spleen collected from mice bearing A498 xenografts. Bar length =200 μm.